THE JOURNAL OF PHYSICAL CHEMISTRY A

Article

pubs.acs.org/JPCA

Influence of N-terminal Residue Composition on the Structure of Proline-Containing b_2^+ Ions

Ashley C. Gucinski,[†,∥] Julia Chamot-Rooke,[‡,⊥] Vincent Steinmetz,[§] Árpád Somogyi,[†] and Vicki H. Wysocki*[,†,#]

[†]Department of Chemistry and Biochemistry, The University of Arizona, 1306 East University Boulevard, P.O. Box 210041, Tucson, Arizona 85721-0041, United States

[‡]Laboratoire des Mecanismes Reactionnels, DCMR, École Polytechnique, Palaiseau 91128, France

[§]Laboratoire de Chimie Physique, Université Paris-Sud 11, Orsay 91405, France

Supporting Information

ABSTRACT: To probe the structural implications of the proline residue on its characteristic peptide fragmentation patterns, in particular its unusual cleavage at its C-terminus in formation of a b_2 ion in XxxProZzz sequences, the structures of a series of proline-containing b_2^+ ions were studied by using action infrared multiphoton dissociation (IRMPD) spectroscopy and fragment ion hydrogen−deuterium exchange (HDX). Five different Xxx-Pro b_2^+ ions were studied, with glycine, alanine, isoleucine, valine, or histidine in the N-terminal position. The residues selected feature different sizes, chain lengths, and gas phase basicities to explore whether the structure of the N-terminal residue influences the Xxx-Pro b_2^+ ion structure. In proteins, the proline side chain-to-backbone attachment causes its peptide bonds to be in the cis conformation more than any other amino acid, although trans is still favored over cis. However, HP is the only b_2^+ ion studied here that forms the diketopiperazine exclusively. The GP, AP, IP, and VP b_2^+ ions formed from protonated tripeptide precursors predominantly featured oxazolone structures with small diketopiperazine contributions. In contrast to the b_2^+ ions generated from tripeptides, synthetic cyclic dipeptides VP and HP were confirmed to have exclusive diketopiperazine structures.

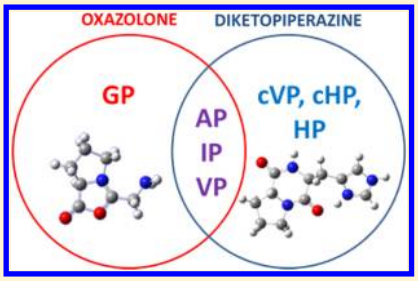

INTRODUCTION

The implementation of mass spectrometry-based techniques for the analysis of peptides and proteins has lead the advancement of proteomics.[1,2] In a typical proteomics experiment, protein samples are enzymatically digested into peptides, which can then be introduced into a mass spectrometer for MS/MS analysis. The presence of peptide fragment ions characteristic of the peptide sequence enable spectra to be assigned to corresponding peptide sequences. However, hundreds to thousands of MS/MS spectra are generated in a standard proteomics experiment, making manual interpretation of each spectrum impractical. To combat this, several protein identification algorithms have been developed to rapidly assign peptide sequences to experimental MS/MS spectra.[3−7] In these algorithms, peptide sequence assignments are made on the basis of comparison between the experimental MS/MS spectra and theoretical MS/MS spectra or peak lists generated from databases of known protein sequences.

Although the advent of protein identification algorithms has greatly accelerated the rate of mass spectral identification, improving the success of these algorithms remains a priority; only a small percentage of all the MS/MS spectra generated in a given experiment are assigned to a peptide sequence.[8] Using the sequence database identification approach, very little chemical information (intensity, enhanced or suppressed peaks) is used in making a peptide identification. One possible way to improve peptide identification algorithms is to incorporate more chemical information describing the peptide fragmentation pathways into the algorithm models. If more is known about how peptides dissociate and what fragment ion structures form, the resulting MS/MS spectra can be more accurately predicted and modeled.[9,10]

The large volume of MS/MS spectra produced in proteomics experiments makes the data aptly suited for analysis by data mining approaches. Data mining can be used to extract trends and patterns from large sets of data. In peptide fragmentation, several groups have used data mining to identify and interpret residue-specific fragmentation behavior.[11−16] Reflecting the importance of the role of the proton in initiating peptide fragmentation, several data mining studies have identified enhanced (and suppressed) cleavages near acidic and basic residues.[4,12−17] Additionally, several groups have also identified a trend of strong enhanced cleavages at the position N-terminal to proline residues; this trend has been reported by several researchers and is known as the 'proline effect'.[2,11−14,18−25]

Huang and co-workers analyzed a data set of 28 330 MS/MS spectra, identifying proton mobility, basic residue position,

Special Issue: Peter B. Armentrout Festschrift

Received: July 8, 2012
Revised: January 10, 2013
Published: January 11, 2013

   dx.doi.org/10.1021/jp306759f | J. Phys. Chem. A 2013, 117, 1291−1298

relative basicity of residues present, and the presence of proline to have the greatest influence on dissociation patterns in MS/MS spectra.[12] This same data set was later analyzed by using a penalized K-means approach, which sorts the data without introducing any initial chemical assumptions.[13] The penalized K-means approach sorted the MS/MS spectra into four clusters with distinctly different behaviors, plus a "noise" cluster of spectra that did not fit the other four clusters; one of the clusters featured peptides with strong cleavage N-terminal to proline residues.[13] The Simpson laboratory used a set of 5500 tryptic peptides to look for amino acid pairs that demonstrated fragmentation enhancement and suppression.[14] Similar to other studies, enhanced cleavage at the position N-terminal to proline were observed. In addition, the work of both Simpson and Huang showed that when the proline residue is the second residue of the peptide, enhanced cleavage at the position C-terminal to proline, not the N-terminal position, was favored.[13,14] In other words, b_2^+ ion formation is favored for peptides featuring Xxx-Pro as the first two residues.

Peptide bond trans−cis isomerization can have a significant effect on large protein crystal structures and peptide b fragment ions alike.[26−28] In peptides, the trans conformation of the peptide bond is highly favored; the cis conformation is only observed in 0.03−0.05% of peptide bonds. The large percentage difference in trans versus cis populations is a result of the large energy differences between the cis and trans isomers for most amino acids, which are on the order of 2.5 kcal/mol, with rotational barriers between the two conformers of approximately 20 kcal/mol.[29−35] For proline, the trans conformation is favored over the cis by only 0.5 kcal/mol, and the rotational barrier between cis and trans is smaller, on the order of 13 kcal/mol.[34]

Although the studies described above have all implemented the use of data mining to identify the trends of the proline effect, relatively few studies have examined the structure of the Xxx-Pro b_2^+ ions. In general, two different b_2^+ ion structures have been well-described: Harrison describes the formation of the oxazolone structure, and Wesdemiotis describes the diketopiperazine structure.[36−38] Eckart and co-workers used a combination of quantum mechanical theoretical calculations and MS/MS experiments to assign the GP b_2^+ ion structure as an oxazolone.[39] Smith and co-workers compared the fragmentation patterns of the synthetic diketopiperazine VP to that of the VP b_2^+ ion generated from the pentapeptide VPAPR to assign the structure of the VP b_2^+ ion as a diketopiperazine.[40] Both of these studies implemented indirect structural techniques to assign a structure to these b_2^+ ions. In MS/MS and MS^3 studies, the structural assignment relies on similarities in fragmentation patterns; however, peptide fragmentation is a complex process, which includes the possibility of interconversion between isomers during the fragmentation process. Additionally, the use of theory alone may also be faulty, as structures alternative to the thermodynamically favored isomer have been found to be present.[41−46] Action IRMPD spectroscopy is a direct structural technique that can provide more accurate structural information, as first reported by Polfer and co-workers for a peptide fragment.[47] In the work presented herein, we use action IRMPD spectroscopy, in complement with hydrogen−deuterium exchange (HDX) and density functional theory (DFT) calculations, to study the influence of N-terminal residue composition on the structure of a series of proline-containing b_2^+ ions. Specifically, the structures of the GP, AP, VP, IP, and HP b_2^+ ions were examined in this study. These residues were chosen to explore influence of side chain size and gas phase basicity on the resulting b_2^+ ion structure(s) formed.

EXPERIMENTAL SECTION

Precursor tripeptides were synthesized in-house using standard solid phase peptide synthesis protocols.[48] Fmoc-protected amino acids were purchased from EMD Biosciences (Gibbstown, NJ). Peptide synthesis coupling reagents and solvents, including HBTU, BOP piperidine, dimethylformamide, and dichloromethane, were purchased from Sigma Aldrich (St. Louis, MO). Diethylamine (DIEA) was purchased from Anaspec (Fremont, CA). Synthetic diketopiperazine dipeptides VP and HP were purchased from Bachem (Torrance, CA). Solid peptides were diluted in 50:50:0.1% water:acetonitrile:formic acid to a concentration of approximately 1−10 μM prior to analysis by using mass spectrometry.

Action IRMPD spectroscopy experiments were performed using the free electron laser (FEL) at the CLIO facility in Orsay, France, as developed by Maître, Ortega, and co-workers, and described previously.[42,44,49−53] Briefly, protonated peptides were generated in a modified Bruker Esquire 3000+ Paul-type ion trap mass spectrometer with an electrospray ionization source. Following mass selection, the isolated precursor ions (protonated tripeptides) were subjected to collision-induced dissociation (CID) using helium to generate the fragment ion of interest. The b_2^+ ions formed by CID were then mass-selected in the ion trap prior to irradiation with the tunable wavelength CLIO free electron laser (FEL) IR beam for 400 ms (i.e., 10 macropulses), which was operated over the range from approximately 1050 to 2050 cm^{-1} using a 4 cm^{-1} step size. The ion is able to absorb photons when the frequency of the laser matches the vibrational frequency of a bond in the ion species; when sufficient photons are absorbed to exceed the bond dissociation threshold, fragmentation is achieved. The relative ratio between the intensity of the fragment ion and precursor ion is used to construct the action IRMPD spectrum, which is plotted with the intensity ratio versus the laser frequency in wavenumbers. As the power of the free electron laser is not uniform over the entire spectral range, all spectra were power corrected using laser power profile curves, consisting of linear fits over each 100 cm^{-1} section of the experimental spectrum.

For comparison to the experimental action IRMPD spectra, theoretical IR spectra were generated from the calculated lowest energy b_2^+ ion structures. Candidate starting structures were generated by using Monte Carlo Conformation Searching simulations using MacroModel (Schrodinger, Inc., Portland, OR). A subset of the generated structures were optimized using DFT calculations at the B3LYP/6-31G and 6-311++G** levels using the Gaussian09 software package.[54] Theoretical spectra were adjusted using a scaling factor of 0.98 with a Lorentzian applied to generate a fwhm resolution of 10 cm^{-1}.

Gas phase fragment ion hydrogen−deuterium exchange (HDX) experiments were performed using a Bruker apex Qe 9.4T FTICR mass spectrometer (Bruker Daltonics, Billerica, MA), as described previously.[42,44,50] Again, protonated peptides were generated by using electrospray ionization. Fragmentation was achieved in the quadrupole region by using quadrupole CID. Following fragmentation, all ions, including any remaining precursor ions, were simultaneously introduced into the ICR cell. Ions were allowed to interact with deuterated methanol (CD_3OD, Cambridge Isotope Laboratories, Andover, MA) at a pressure of 200 mbar for a variety of different pulse lengths to

examine the gas phase exchange profiles, including extent of exchange and relative exchange rate, of the fragment ions.

RESULTS/DISCUSSION

Because both thermodynamically and kinetically favored products can be formed in a mass spectrometer, the relationship between the relative thermodynamic stability of the different possible fragment ion isomers should be explored to understand which factor is driving the fragmentation process. To determine which b_2^+ ion structure is thermodynamically favored for each b_2^+ ion sequence, the relative free energies of the lowest energy diketopiperazine and oxazolone structures were obtained, as summarized in Table 1. Without exception, the six-membered ring diketopiperazine structure is lower in energy than the five-membered ring oxazolone structure of the same sequence. Though the energy differences between the oxazolone and diketopiperazine are approximately the same (~55 kJ/mol) for aliphatic N-terminal residues, the presence of the basic N-terminal histidine residue results in a significantly more stable diketopiperazine structure (132.2 kJ/mol versus ~50 kJ/mol).

Table 1. Summary of Relative Oxazolone and Diketopiperazine Free Energies for Xxx-Pro b_2^+ Ion Structures

b_2^+ ion	oxazolone (kJ/mol)	diketopiperazine (kJ/mol)
GP	47.7	0
AP	55.5	0
VP	58.5	0
IP	54.4	0
HP	132.2	0

The b_2^+ ion with the smallest N-terminal residue, glycine, was generated from the protonated tripeptide GPA. The resulting action IRMPD spectrum of the GP b_2^+ ion is shown in Figure 1, along with theoretical spectra corresponding to the calculated lowest energy oxazolone and diketopiperazine structures. The GP b_2^+ ion presents excellent agreement with the theoretical oxazolone IR spectrum. Table 2 summarizes the experimental and predicted IR modes for the GP b_2^+ ion. Experimentally observed bands were consistent with theoretically predicted values for the oxazolone structure, including the C═O stretch at 1950 cm^{-1}, the C═N stretch at 1640 cm^{-1}, and the C—O stretch at 1315 cm^{-1}. The free N-terminus, as indicated by the NH_2 scissoring mode observed at 1660 cm^{-1} (and synchronously with the oxazolone C═N stretch at 1640 cm^{-1}) further supports this assignment, consistent with the identification made by Eckart and co-workers based on data from CID and HDX experiments in combination with DFT calculations.[39] In addition to the presence of a free N-terminus, the absence of the characteristic diketopiperazine amide I stretches, expected at 1771 and 1679 cm^{-1}, further suggests that the GP diketopiperazine is not present.

The GP b_2^+ ion was also analyzed by using fragment ion HDX and the exchange profile is shown in Figure 2, left column. Even after long exchange times, no deuterium incorporates into the fragment ion. Although the lack of exchange may reflect a single population incapable of exchange, multiple populations, if present, could also be incapable of exchange so lack of exchange does not distinguish these possibilities. The backbone attachment of the proline side chain introduces steric strain into the fragment ion structure; the bicyclic structures of both the diketopiperazine and oxazolone structures impose rigidness on the overall b_2^+ ion structures. Because CD_3OD undergoes exchange via the relay mechanism,[55,56] requiring the deuterating reagent to bridge between two basic sites within the molecule, the geometric constraints may prohibit exchange in either b_2^+ ion structure. Though the amino terminus of the oxazolone does feature two potentially exchangeable hydrogens, there is no bridging site of comparable basicity to participate in the relay mechanism.

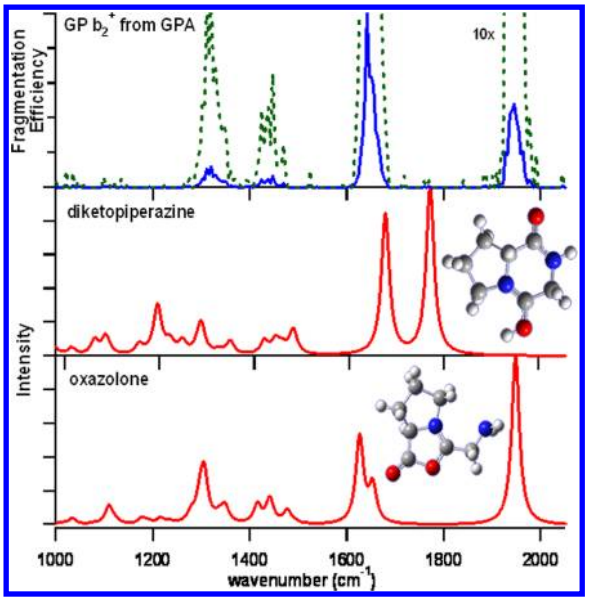

Figure 1. Action IRMPD spectrum of the GP b_2^+ ion generated from the protonated tripeptide GPA. Theoretical diketopiperazine (middle) and oxazolone (bottom) spectra, corresponding to the overlaid lowest energy structures calculated at the 6-311++G** level, are shown for comparison. A 10-fold magnified experimental spectrum is shown in dashed green.

The action IRMPD spectrum of the b_2^+ ion with the next largest side chain structure, AP, as generated from the protonated tripeptide APA, is shown in Figure 3. The lowest energy AP b_2^+ ion structures, also shown in Figure 3, feature the same orientation of the side chain relative to the oxazolone ring and the same protonation sites for both structural isomers as in the GP b_2^+ ion, with only the addition of the methyl group differentiating between the two sets of structures. Similar to the GP spectrum, the predominant structure in the AP action IRMPD spectrum reflects an oxazolone structural population. A summary of the observed modes is shown in Table 3. However, upon a 50-fold magnification of the experimental spectrum, prominent stretches at ~1700 and 1770 cm^{-1}, corresponding to the unprotonated and protonated amide CO stretches, respectively, mark the presence of an additional diketopiperazine population for the AP b_2^+ ion. Although additional stretches corresponding the diketopiperazine structure may also be present, the broad, more dominant oxazolone stretches dominate the spectrum in those regions, preventing additional diketopiperazine IR stretches from being observed. In relation to the GP system, the increased side chain size may introduce some additional steric strain in the available rotations and conformations of the first peptide bond.

Fragment ion HDX was performed on the AP b_2^+ ion, as shown in Figure 2, to determine if exchange populations representing both the oxazolone and diketopiperazine structures could be identified. Similar to the GP system, no

dx.doi.org/10.1021/jp306759f | J. Phys. Chem. A 2013, 117, 1291−1298

Table 2. Summary of 6-311++G Predicted (Shown in Parentheses) and Experimentally Observed IR Modes for the GP, AP, VP, and IP b_2^+ Ions**

experimental frequency (cm^{-1}) (theoretical frequency, (cm^{-1}))				
GP	AP	VP	IP	description
		Oxazolone Stretches		
1950 (1951)	1940 (1948)	1926 (1942)	1937 (1941)	C═O stretch
1660 (1649)	1638 (1644)	broad (1639)	broad (1639)	NH_2 scissoring
1640 (1622)	1623 (1614)	1608 (1600)	broad (1606)	C═N stretch with NH_2 scissoring
1315 (1293)	1310 (1283)	broad (1300)	broad (1298)	C−O stretch with C−H symmetric stretch
		Diketopiperazine Stretches		
N/A (1771)	1770 (1771)	1760 (1763)	1760 (1757)	amide I C═O stretch
N/A (1679)	1700 (1699)	1701 (1700)	1676 (1666)	protonated amide C═O stretch
N/A (1489)	N/A (1492)	broad (1461)	broad (1475)	amide II N−H rocking
N/A (1209)	N/A (1194)	broad (1224)	N/A (1213)	protonated carbonyl C═O−H + OH stretch

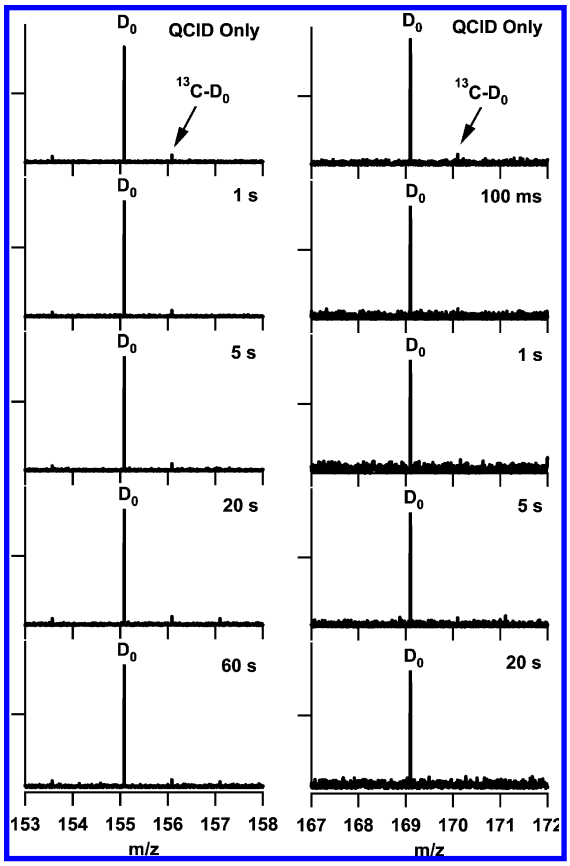

Figure 2. HDX behavior of the (left) GP and AP (right) b_2^+ ions. Exchange time points increase downward, as labeled. The QCID only (no exchange) spectrum is shown at the top to show the presence of the ^{13}C isotopomer of the D_0 population and not a D_1 population, as confirmed by mass defect analysis.

exchange occurs, likely as a result of the structural rigidity of the AP b_2^+ ion bicyclic structure, impeding the deuterated methanol from achieving the geometry necessary to bridge within the fragment ion. Although this result does not negate the presence of two populations, it demonstrates that this HDX system (i.e., exchange with CD_3OD at 200 mbar) cannot be used to confirm (or negate) the presence of multiple structural populations for this system.

To continue exploring the effect of side chain size on Xxx-Pro b_2^+ ion structures, the action IRMPD spectrum for the VP b_2^+ ion from the protonated tripeptide VPA was obtained, as shown in Figure 4. The action IRMPD spectrum for protonated synthetic diketopiperazine VP ion was also acquired for comparison. Similar to GP and AP, the dominant VP b_2^+ ion structure is an oxazolone, as marked by the characteristic oxazolone C═O stretch at ~1930 cm^{-1}. Further confirmation of this structural identification is supported by the presence of the NH_2 wagging modes, both alone and with the oxazolone ring C═N stretch, which are found at ~1630 and 1660 cm^{-1}; however, the spectral resolution obtained in this experiment results in the overlap of these stretches. Similar to the previously discussed systems and according to the calculations (see low energy structures in Figure 4), the oxazolone N-terminal nitrogen is rotated toward the proline nitrogen which has a formal charge of 1^+, whereas the diketopiperazine, protonated on the amide carbonyl, features the proton rotated toward the alkyl side chain moiety.

Similar to the case for the AP b_2^+ ion, magnification of the VP b_2^+ ion experimental spectrum reveals the presence of stretches corresponding to the lowest energy diketopiperazine structure. The characteristic amide C═O stretches are present at 1765 and 1705 cm^{-1}, and the amide NH wagging mode is present at approximately 1517 cm^{-1}. The second amide NH wagging mode cannot be discerned because of overlapping oxazolone stretches dominating the spectrum in that region. The identification of the VP b_2^+ ion as predominantly an oxazolone conflicts with the results from MS/MS and MS^3 experiments performed by Smith and co-workers on both the VP b_2^+ ion and the cyclic commercial VP diketopiperazine, who assigned the VP b_2^+ ion structure as predominantly diketopiperazine.[40] Differences between the structural assignment made by using action IRMPD data versus indirect MS/MS and MS^3 data suggests that the interpretation of MS^n data alone is inadequate for structural assignment. This result is similar to that seen for the HA and HG systems, in which MS/MS and MS^3 fragmentation patterns and DFT calculations led O'Hair and co-workers to identify the HG and GH systems as diketopiperazines, whereas spectroscopic results for the very similar HA system identified a mixture of oxazolone and diketopiperazine populations for that b_2^+ ion.[42,44,57] Similar to HG and GH, the VP diketopiperazine is lower in energy than the VP oxazolone (by 58.5 kJ/mol). Despite the diketopiperazine being the thermodynamically favored structure, the kinetically favored oxazolone dominates the action IRMPD spectrum. These results further demonstrate the need for direct structural techniques to be used for the determination of peptide fragment ion structure.

The action IRMPD spectrum of the protonated synthetic diketopiperazine VP (cVP) was also acquired and shown in

dx.doi.org/10.1021/jp306759f | J. Phys. Chem. A 2013, 117, 1291−1298

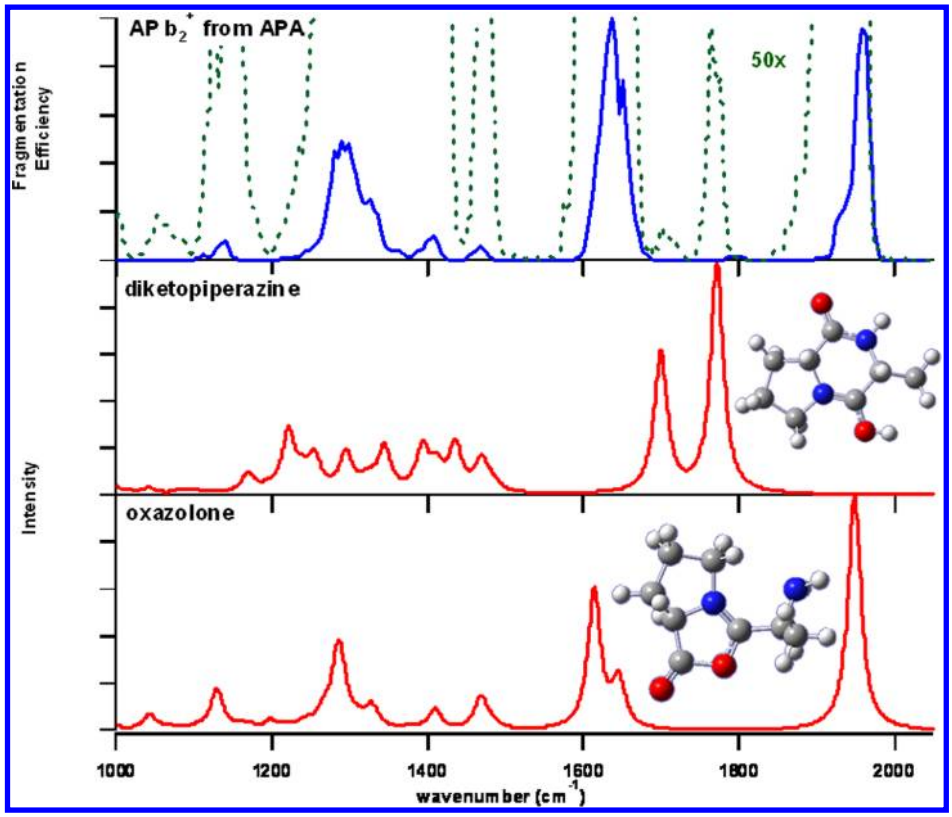

Figure 3. Action IRMPD spectrum of the AP b_2^+ ion. Calculated IR spectra from lowest energy diketopiperazine (middle) and oxazolone (bottom) structures are shown for comparison. A 50-fold magnification of the experimental spectrum is shown to highlight the diketopiperazine contribution.

Table 3. Summary of 6-311++G Predicted and Experimentally Observed IR Modes for the HP b_2^+ Ion System**

theoretical frequency (cm^{-1})	description	experimental frequency (cm^{-1})
	Oxazolone Stretches	
1871	oxazolone C═O stretch	N/A
1690	NH_2 scissoring, N terminus	N/A
1622	oxazolone C═N stretch	N/A
	Diketopiperazine Stretches	
1755	amide I C═O stretch	1760
1656	amide I C═O stretch, protonated with histidine ring breathing	1665
1614	histidine ring breathing	1610

Figure 4. The experimental spectrum features strong agreement with both the theoretical diketopiperazine IR spectrum and the diketopiperazine amide stretches seen in the VP b_2^+ ion action IRMPD spectrum generated from the VPA precursor. A comparison of the b_2^+ ion H/D exchange profiles, as shown in Figure 5, shows a distinct difference for the cVP structure versus the ion generated from the tripeptide precursor. No deuterium is incorporated for VP b_2^+ ion generated from the tripeptide precursors, even after long periods of exchange. In contrast, the cVP ion shows the slow incorporation of one deuterium atom, further supporting the fact that different b_2^+ ion structural populations are formed from cVP versus protonated VPA.

Results similar to those of VP were seen for the IP b_2^+ ion generated from the IPA tripeptide precursor, with a predominant oxazolone and a trace diketopiperazine structural

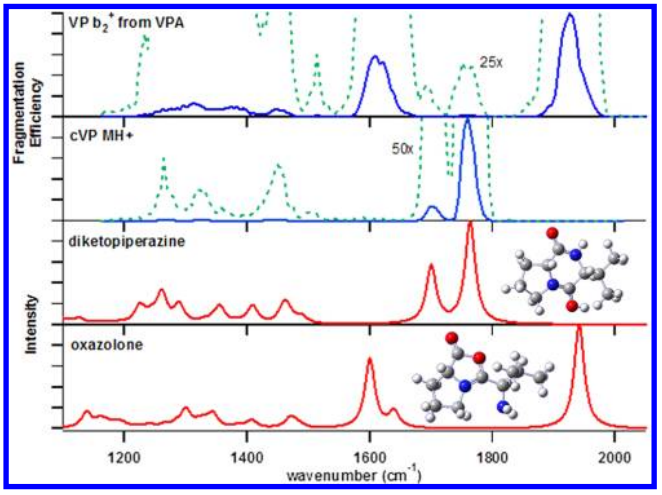

Figure 4. Action IRMPD spectra of the (a) VP b_2^+ ion generated from the protonated tripeptide VPA and (b) the protonated synthetic diketopiperazine VP (cVP). Magnifications of the experimental spectra are shown in the dashed green line overlaid on each experimental spectrum. Lowest energy (c) diketopiperazine and (d) oxazolone structures are shown for comparison.

population both being identified (Supporting Information). The fragment ion HDX profile of IP is shown alongside the VP b_2^+ ion and cVP HD exchange in Figure 5, whereas the action IRMPD spectrum and corresponding calculated lowest-energy ion structures and theoretical IR spectra, are shown in the Supporting Information, Figure S1. In contrast to AP, GP, and VP, two deuterium atoms are seen to incorporate into the IP b_2^+ ion structure. Though two potentially exchangeable amino terminal hydrogens are present in the oxazolone structure for

dx.doi.org/10.1021/jp306759f | J. Phys. Chem. A 2013, 117, 1291−1298

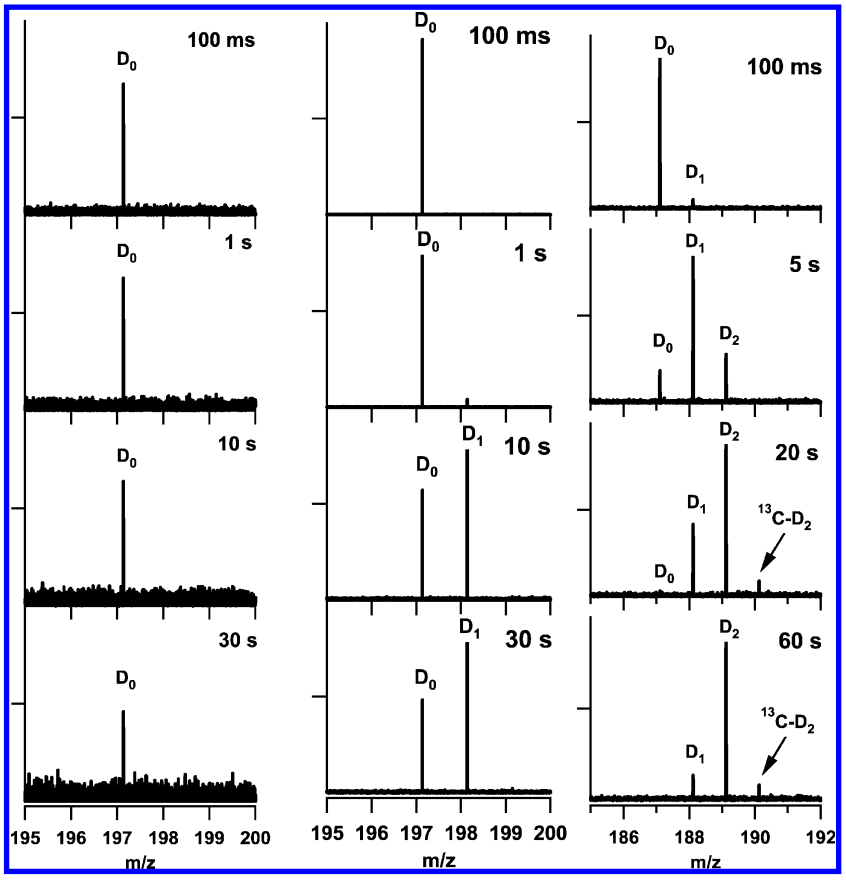

Figure 5. HDX behavior of the VP b_2^+ ion (left), protonated cyclic diketopiperazine VP (middle), and IP b_2^+ ion (right). Exchange time increases from top to bottom of the figure.

all three b_2^+ ions, the increased size and length of the isoleucine side chain may impose a structural influence that alters the ion structure in a manner that more readily facilitates bridging and thus exchange (e.g., rotating the amino terminus "down" toward the oxazolone ring oxygen). More research is needed to fully explain this contrast in behavior.

To probe the influence of a basic residue on the structure of a Xxx-Pro b_2^+ ion, the HP b_2^+ ion structure was also studied. Previous structural studies of histidine containing b_2^+ ions have been performed on the HA system.[42,44] Ion contrast to the purely oxazolone AA b_2^+ ion,[43] the HA b_2^+ ion features a mixture of both oxazolone and diketopiperazine b_2^+ ion structures. All of the other Xxx-Pro b_2^+ ion structures studied thus far in this work have favored formation of the oxazolone structure, despite the somewhat higher propensity for proline to be in the cis conformation, compared with other amino acids, and the fact that the diketopiperazine structure is always energetically favored to the oxazolone for these systems. The action IRMPD spectra of the protonated diketopiperazine cHP and the HP b_2^+ ion from the protonated tripeptide HPA are shown in Figure 6, along with the two lowest energy HP diketopiperazine isomers and lowest energy oxazolone structure. Both diketopiperazine structures are protonated on the histidine side chain imidazole nitrogen but feature different relative angles between the diketopiperazine and histidine side chain rings (the rings are parallel in the lowest energy structure and are angled toward each other in the higher energy structure). The change in the angles between the rings causes the relative intensity of the histidine ring breathing mode and the stretch of the concerted histidine ring breathing mode and

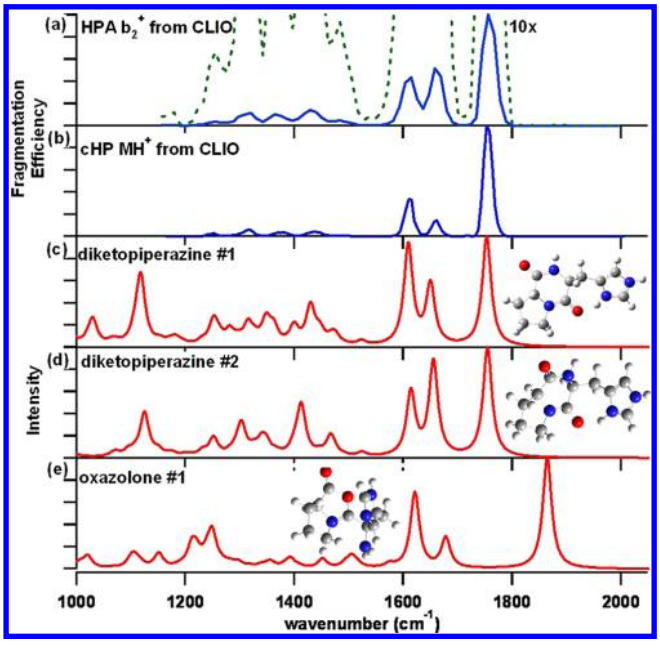

Figure 6. Action IRMPD spectra of the (a) b_2^+ ion from protonated HPA and (b) protonated diketopiperazine HP. Magnifications of the experimental spectrum in (a) are shown in the dashed green line overlay. The two calculated lowest-energy diketopiperazine (c, d) and oxazolone (e) spectra, along with their corresponding structures, are shown for comparison.

dx.doi.org/10.1021/jp306759f | J. Phys. Chem. A 2013, 117, 1291−1298

the protonated C═O amide stretch to change. The difference in relative intensity of the experimental spectrum compared to either of the two lowest HP b_2^+ ion structures suggests that the HP b_2^+ ion has both diketopiperazine structures present. In contrast, the oxazolone structure has the charge fixed on the proline nitrogen. The predominant modes observed along with the expected theoretical frequencies are summarized in Table 3.

Unlike the aliphatic side chain systems, no stretches corresponding to the oxazolone structure are seen in the IRMPD spectra of the cyclic diketopiperazine HP or the b_2^+ ion from HPA; only IR stretches at frequencies corresponding to the diketopiperazine structure are seen. In the case of HA, the availability of the π nitrogen as a protonation/bridging site facilitates diketopiperazine formation, whereas the size of the side chain prevents exclusive formation of the diketopiperazine, so the oxazolone structure is also present. However, because the energy difference between the cis and trans isomers is relatively small for proline (with a smaller rotational barrier than for all other amino acids), the peptide bond is likely able to isomerize to the cis conformation because of both the presence of the second position proline and the influence of the histidine nitrogen to also facilitate the isomerization to the cis conformation. The large energy difference between the diketopiperazine and oxazolone for the HP system (oxazolone is 132.2 kcal/mol higher in energy for HP, compared to 85.7 kJ/mol for HA and 55.5 kJ/mol for AP) may also contribute to the diketopiperazine structure of this system. HDX was also performed on the cyclic HP and HP b_2^+ ion systems, as shown in Figure 7. Both the protonated diketopiperazine and the b_2^+ ion formed from the polypeptide feature the slow incorporation of one deuterium atom, in accord with the exchange behavior exhibited by all other diketopiperazine structures previously studied. The HP b_2^+ ion is able to reach the same amount of the D_1 population after 30 s as requires 60 s for the cyclic HP structure. The exchange behavior cannot provide accurate kinetic rate information using the pulsed valve exchange setup; the pattern of deuterium incorporation and relative rate are similar for the cyclic HP and HP b_2^+ ions, further supporting the HP b_2^+ ion identification as a diketopiperazine structure. The exchange of one proton for the cyclic HP diketopiperazine is consistent with the results for the HA diketopiperazine, where the CD_3OD likely inserts between the protonated imidazole and the diketopiperazine ring amide carbonyl group for exchange to occur.[44]

CONCLUSIONS

A series of Xxx-Pro b_2^+ ions were studied by action IMRPD spectroscopy, fragment ion hydrogen−deuterium exchange, and DFT calculations to determine the fragment ion structures. Xxx with aliphatic N-terminal residues produce exclusive or predominant oxazolone b_2^+ ion structures. When the basic residue histidine is in the N-terminal position, an exclusive diketopiperazine structure is observed. The HP b_2^+ ion structure is reflective of both the histidine and proline residues, as the HA b_2^+ ion features a mixture of oxazolone and diketopiperazine structures; the conformational constraint of the proline side chain, in contrast to the small alanine side chain, shifts the fragmentation product ion to an exclusive diketopiperazine structure. These results are important not only to obtain a more complete understanding of the peptide fragmentation process in the presence of proline residues but also to reinforce the fact that MS/MS data alone are inadequate for the structural identification of peptide ion structures.

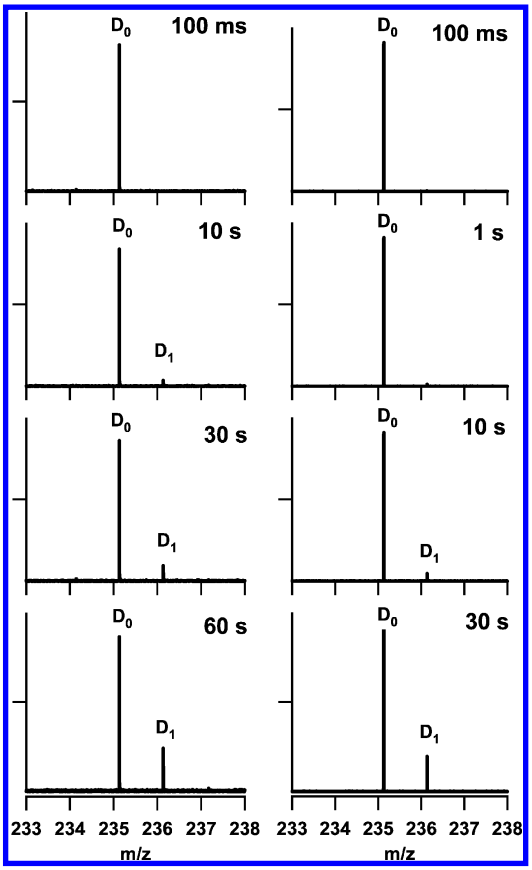

Figure 7. Fragment Ion HDX of the b_2^+ ions from protonated HPA (left) and cyclo-HP (right). Exchange time increases from top to bottom panel.

Whereas fragment ion HDX was attempted for all the systems, the use of CD_3OD, which has been shown to undergo HDX via the relay mechanism, was unable to incorporate any deuterium atoms into many of the Xxx-Pro b_2^+ ion systems (IP and HP as exceptions). The use of alternative, less conformationally selective deuterating agents such as NH_3 may provide more useful exchange data that can corroborate or negate the results seen from the action spectroscopy.

ASSOCIATED CONTENT

Supporting Information

Action IRMPD spectrum for the IP b_2^+ ion and magnifications of all calculated lowest-energy structures and their corresponding *xyz* coordinates, along with the complete citations for refs 53 and 54. This information is available free of charge via the Internet at http://pubs.acs.org

AUTHOR INFORMATION

Corresponding Author

*E-mail: wysocki.11@chemistry.ohio-state.edu. Phone (614) 292-8687.

Present Addresses

[‖]Division of Pharmaceutical Analysis, U.S. Food and Drug Administration, 1114 Market St., Saint Louis, MO, United States. E-mail: ashley.gucinski@fda.hhs.gov.

[⊥]Institut Pasteur, 25-28 rue du Dr Roux, Paris cedex 15, Paris 75724, France.

[#]The Ohio State University, 484 W. 12th Ave., Columbus, OH 43210, United States.

Notes

The authors declare no competing financial interest.

■ ACKNOWLEDGMENTS

The authors gratefully acknowledge the aid and expertise of the CLIO facility support staff, J. Lemaire, P. Maître, B. Rieul, R. Singha, and C. Six. Fellowship support from the French Embassy of the US, Office of Science and Technology, awarded to A.C.G. is gratefully acknowledged. Funding from NIH GM R01 51387 awarded to V.H.W. is gratefully acknowledged.

■ REFERENCES

(1) Aebersold, R.; Mann, M. *Nature* **2003**, *422*, 198−207.
(2) Hunt, D. F.; Yates, J. R.; Shabanowitz, J.; Winston, S.; Hauer, C. R. *Proc. Nat. Acad. Sci. U. S. A.* **1986**, *83*, 6233−6237.
(3) Craig, R.; Beavis, R. C. *Bioinformatics* **2004**, *20*, 1466−1467.
(4) Elias, J. E.; Gibbons, F. D.; King, O. D.; Roth, F. P.; Gygi, S. P. *Nat. Biotechnol.* **2004**, *22*, 214−219.
(5) Eng, J. K.; McCormack, A. L.; Yates, J. R. *J. Am. Soc. Mass Spectrom.* **1994**, *5*, 976−989.
(6) Li, W.; Ji, L.; Goya, J.; Tan, G.; Wysocki, V. *J. Proteome Res.* **2011**, *10*, 1593−1602.
(7) Perkins, D. N.; Pappin, D. J.; Creasy, D. M.; Cottrell, J. S. *Electrophoresis* **1999**, *20*, 3551−3567.
(8) Nesvizhskii, A. E.; Vitek, O.; Aebersold, R. *Nat. Methods* **2007**, *4*, 787−797.
(9) Wysocki, V. H.; Resing, K. A.; Zhang, Q.; Chang, G. L. *Methods* **2005**, *35*, 211−222.
(10) Wysocki, V. H.; Tsaprailis, G.; Smith, L. L.; Breci, L. A. *J. Mass Spectrom.* **2000**, *35*, 1399−1406.
(11) Breci, L. A.; Tabb, D. L.; Yates, J. R., III; Wysocki, V. *Anal. Chem.* **2003**, *75*, 1963−1971.
(12) Huang, Y.; Triscari, J. M.; Tseng, G. C.; Pasa-Tolic, L.; Lipton, M. S.; Smith, R. D.; Wysocki, V. H. *Anal. Chem.* **2005**, *77*, 5800−5813.
(13) Huang, Y.; Tseng, G. C.; Yuan, S.; Pasa-Tolic, L.; Lipton, M. S.; Smith, R. D.; Wysocki, V. *J. Proteome Res.* **2008**, *7*, 70−79.
(14) Kapp, E. A.; Schutz, F.; Reid, G. E.; Eddes, J. S.; Moritz, R. L.; O'Hair, R. A. J.; Speed, T. P.; Simpson, R. J. *Anal. Chem.* **2003**, *75*, 6251−6264.
(15) Tabb, D. L.; Huang, Y.; Wysocki, V.; Yates, J. R., III. *Anal. Chem.* **2004**, *76*, 1243−1248.
(16) Tabb, D. L.; Smith, L. L.; Breci, L. A.; Wysocki, V. H.; Lin, D.; Yates, J. R. *Anal. Chem.* **2003**, *75*, 1155−1163.
(17) Huang, Y. Y.; Wysocki, V. H.; Tabb, D. L.; Yates, J. R., III. *Int. J. Mass Spectrom.* **2002**, *219*, 233−244.
(18) Loo, J. A.; Edmonds, C. G.; Smith, R. D. *Anal. Chem.* **1993**, *65*, 425−438.
(19) Martin, S. A.; Biemann, K. *Int. J. Mass Spectrom. Ion Processes* **1987**, *78*, 213−228.
(20) Tang, X. J.; Thibault, P.; Boyd, R. K. *Anal. Chem.* **1993**, *65*, 2824−2834.
(21) Vaisar, T.; Urban, J. *J. Mass Spectrom.* **1996**, *31*, 1185−1187.
(22) Bleiholder, C.; Suhai, S.; Harrison, A. G.; Paizs, B. *J. Am. Soc. Mass Spectrom.* **2011**, *22*, 1032−1039.
(23) Grewal, R. N.; El Aribi, H.; Harrison, A. G.; Siu, K. W. M.; Hopkinson, A. C. *J. Phys. Chem. B* **2004**, *108*, 4899−4908.
(24) Schwartz, B. L.; Bursey, M. M. *Biol. Mass Spectrom.* **1992**, *21*, 92−96.
(25) Unnithan, A. G.; Myer, M. J.; Veale, C. J.; Danell, A. S. *J. Am. Soc. Mass Spectrom.* **2007**, *18*, 2198−2203.
(26) Paizs, B.; Suhai, S. *Rapid Commun. Mass Spectrom.* **2001**, *15*, 2307−2323.
(27) Paizs, B.; Suhai, S. *Rapid Commun. Mass Spectrom.* **2002**, *16*, 375−389.
(28) Reimer, U.; Scherer, G.; Drewello, M.; Kruber, S.; Schutkowski, M.; Fischer, G. *J. Mol. Biol.* **1998**, *294*, 271−288.
(29) Jabs, A.; Weiss, M. S.; Hilgenfeld, R. *J. Mol. Biol.* **1999**, *286*, 291−304.
(30) Jorgensen, W. L.; Gao, J. *J. Am. Chem. Soc.* **1988**, *110*, 4212−4216.
(31) LaPlanche, L. A.; Rogers, M. T. *J. Am. Chem. Soc.* **1964**, *86*, 337−341.
(32) MacArthur, M. W.; Thornton, J. M. *J. Mol. Biol.* **1991**, *218*, 397−412.
(33) Maigret, B.; Perahia, D.; Pullman, B. *J. Theor. Biol.* **1970**, *29*, 275−291.
(34) Pal, D.; Chakrabarti, P. *J. Mol. Biol.* **1999**, *294*, 271−288.
(35) Stewart, D. E.; Sarkar, A.; Wampler, J. E. *J. Mol. Biol.* **1990**, *214*, 253−260.
(36) Harrison, A. G. *Mass Spectrom. Rev.* **2009**, *28*, 640−654.
(37) Nold, M. J.; Wesdemiotis, C.; Yalcin, T.; Harrison, A. G. *Int. J. Mass Spectrom. Ion Processes* **1997**, *164*, 137−153.
(38) Yalcin, T.; Khouw, C.; Csizmadia, I. G.; Peterson, M. R.; Harrison, A. G. *J. Am. Soc. Mass Spectrom.* **1995**, *7*, 233−242.
(39) Eckart, K.; Holthausen, M. C.; Koch, W.; Spiess, J. *J. Am. Soc. Mass Spectrom.* **2006**, *17*, 20−28.
(40) Smith, L. L.; Herrmann, K. A.; Wysocki, V. H. *J. Am. Soc. Mass Spectrom.* **2006**, *17*, 20−28.
(41) Bythell, B. J.; Somogyi, A.; Paizs, B. *J. Am. Soc. Mass Spectrom.* **2009**, *20*, 618−624.
(42) Gucinski, A. C.; Chamot-Rooke, J.; Nicol, E.; Somogyi, A.; Wysocki, V. *J. Phys. Chem. A* **2011**, 116.
(43) Oomens, J.; Young, S.; Molesworth, S.; van Stipdonk, M. *J. Am. Soc. Mass Spectrom.* **2009**, 334−339.
(44) Perkins, B. R.; Chamot-Rooke, J.; Yoon, S. H.; Gucinski, A. C.; Somogyi, A.; Wysocki, V. *J. Am. Chem. Soc.* **2009**, *131*, 17528−17529.
(45) Ranasinghe, A.; Cooks, R. G.; Sethi, S. K. *Org. Mass Spectrom.* **1992**, *27*, 77−88.
(46) Yoon, S. H.; Chamot-Rooke, J.; Perkins, B. R.; Hilderbrand, A. E.; Poutsma, J. C.; Wysocki, V. H. *J. Am. Chem. Soc.* **2008**, *130*, 17644−17645.
(47) Polfer, N. C.; Oomens, J.; Suhai, S.; Paizs, B. *J. Am. Chem. Soc.* **2005**, *127*, 17154−17155.
(48) Atherton, E.; Sheppard, R. C. *Solid-Phase Peptide Synthesis: A Practical Approach*; Oxford University Press: Oxford, U.K., 1989.
(49) Bagratashvili, V. N.; Letokov, V. S.; Makarov, A. A.; Ryabov, E. A. *Multiple Photon Infrared Laser Photophysics and Photochemistry*; Harwood: Chichester, U.K., 1985.
(50) Gucinski, A. C.; Somogyi, A.; Chamot-Rooke, J.; Wysocki, V. H. *J. Am. Soc. Mass Spectrom.* **2010**, *21*, 1329−1338.
(51) Lemaire, J.; Boissel, P.; Heninger, M.; Mauclaire, G.; Bellec, G.; Mestdagh, H.; Simon, A.; Le Caer, S.; Ortega, J. M.; Glotin, F.; Maitre, P. *Phys. Rev. Lett.* **2002**, *89*, 273002/273001−273002/273004.
(52) Mac Aleese, L.; Simon, A.; McMahon, T. B.; Ortega, J.; Scuderi, D.; Lemaire, J.; Maitre, P. *Int. J. Mass Spectrom.* **2006**, *249*−*250*, 14−20.
(53) Maitre, P.; Le Caer, S.; Simon, A.; Jones, W.; Lemaire, J.; Mestdagh, H.; Heninger, M.; Mauclaire, G.; Boissel, P.; Prazeres, R.; et al. *Nucl. Instrum. Methods Phys. Res., Sect. A* **2003**, *507*, 541−546.
(54) Frisch, M. J.; Trucks, G. W.; Schlegel, H. B.; Scuseria, G. E.; Robb, M. A.; Cheeseman, J. R.; Scalmani, G.; Barone, V.; Mennucci, B.; Petersson, G. A.; et al. *Gaussian*; Gaussian, Inc.: Wallingford, CT, 2009.
(55) Campbell, S.; Rodgers, M. T.; Marzluff, E. M.; Beauchamp, J. L. *J. Am. Chem. Soc.* **1994**, *116*, 9765−9766.
(56) Campbell, S.; Rodgers, M. T.; Marzluff, E. M.; Beauchamp, J. L. *J. Am. Chem. Soc.* **1995**, *117*, 12840−12854.
(57) Farrugia, J. M.; Taverner, T.; O'Hair, R. A. J. *Int. J. Mass Spectrom.* **2001**, *209*, 99−112.